Repeated Index Modulation-OFDM with Coordinate Interleaving: Performance Optimization and Low-Complexity Detectors

Thi Thanh Huyen Le, *Non-Member*, Xuan Nam Tran, Vu-Duc Ngo, Minh-Tuan Le, *Member, IEEE*

***Abstract*—This paper investigates performance of an advanced scheme of index modulation for orthogonal frequency division multiplexing (IM-OFDM), called the repeated index modulation-OFDM with coordinate interleaving (RIM-OFDM-CI), which achieves higher transmission reliability than the conventional IM-OFDM with coordinate interleaving (IM-OFDM-CI). We first derive the approximated expressions for the symbol error probability (SEP) of RIM-OFDM-CI. The obtained SEP provides an insight into the impact of system parameters on the error performance, which allows for selection of an optimum constellation rotation angle to minimize SEP. Two enhanced detectors, namely the log likelihood ratio (LLR) and greedy (GD) detector for RIM-OFDM-CI are proposed. The proposed detectors not only achieve nearly same performance as the maximum likelihood (ML) detector but also significantly reduce detection complexity of the RIM-OFDM-CI system. Simulation results are reported to validate advantages of the proposed RIM-OFDM-CI and low-complexity detectors against benchmarks.**

Keywords*—*IM-OFDM, coordinate interleaving, symbol error probability, ML detection, log likelihood ratio, greedy detection.

I. Introduction

Index modulation for orthogonal frequency division multiplexing (IM-OFDM) is an effective transmission scheme in the frequency domain as it not only attains higher energy efficiency but also more reliability than the conventional OFDM. Different from the classical OFDM, the IM-OFDM system activates only a fraction of sub-carriers for transmission and uses their indices to convey additional data bits.

The original IM-OFDM system [1] used a fixed number of data bits to activate the corresponding sub-carriers and thus its spectral efficiency and error performance are limited. In order to obtain the flexible trade-off between the transmission reliability and spectral efficiency, the authors in [2] proposed an enhanced IM-OFDM scheme with adjustable active sub-carriers according to incoming bits. In order to deal with the error performance issue, the sub-carriers are interleaved in [3] to extend the Euclidean distance among the data symbols. The study in [4] used interleaved sub-carrier grouping and investigated the achievable rate of the IM-OFDM system.

To improve the spectral efficiency, the work in [5] proposed an IM-OFDM scheme in both in-phase/quadrature (IM-OFDM-I/Q) dimensions, which performs index modulation over both the in-phase and quadrature components of the modulated symbols. In another solution, the dual-mode OFDM (DM-OFDM) was presented in [6]. This model utilized inactive sub-carriers to carry further data bits in addition to the active sub-carriers. Different signal constellations were employed to convey data symbols over both active and inactive sub-carriers. The work in [7] introduced a multi-mode IM-OFDM scheme which activates all sub-carriers. More information bits can be conveyed by permuted transmission modes and thus this scheme can enjoy further increased spectral efficiency. In order to achieve both spectral efficiency and diversity gain, the authors in [8] introduced a linear constellation precoder for IM-OFDM. In another effort, the study in [9] applied the compressed sensing technique to IM-OFDM to attain performance enhancement with respect to both diversity gain and energy efficiency.

Recently, various researches have also been done to analyze performance of IM-OFDM. The work in [10] derived a tight bound for bit error rate (BER) of IM-OFDM. The authors in [11] evaluated the outage probability of the IM-OFDM scheme operating over the two-way diffused-power fading channels. The reliability in terms of symbol error probability (SEP) of IM-OFDM and IM-OFDM employing greedy detection under imperfect channel state information (CSI) was investigated in [12] and [13], respectively.

Aiming at achieving diversity gain, the coordinate interleaved IM-OFDM scheme in [14] distributed the real and imaginary components of the M-ary modulated symbols over distinctive sub-carriers. Paper [15] introduced an IM-OFDM scheme with transmit diversity, which utilized multiple signal constellations to carry the same data bits over the active sub-carriers. In a recent work [16], the coded IM-OFDM with transmit diversity was proposed to increase the reliability of sub-carrier index detection. To achieve further diversity gain and BER performance improvement, the IM-OFDM concept was extended to multiple-input multiple-output (MIMO) systems in [17], [18]. In order to reduce complexity while still attaining diversity gain of IM-OFDM, the study in [19] introduced an IM-OFDM system with greedy detection and diversity reception. Its BER performance under imperfect CSI was analyzed in [20]. A repeated IM-OFDM system with

Dr. Thi Thanh Huyen Le and Prof. Xuan Nam Tran are with the Advanced Wireless Communications Group, Le Quy Don Technical University, 236 Hoang Quoc Viet, Bac Tu Liem, Ha Noi, Viet Nam, e-mail: huyen.ltt@mta.edu.vn, namtx@mta.edu.vn).

Dr. Vu-Duc Ngo is with School of Electronics and Telecommunication, Hanoi University of Science and Technology, Hanoi, Viet Nam, e-mail: duc.ngovu@hust.edu.vn and Dr. Minh-Tuan Le is with MobiFone R&D Center, MobiFone Corporation, VP1 Lot, Yen Hoa, Cau Giay, Hanoi, Viet Nam, e-mail: tuan.minh@mobifone.vn.

transmit diversity (ReMO) was presented in [21] with the closed-form expressions for SEP and BER.

In order to reduce the detection complexity of index modulation systems, the authors in [22], [23], [24] proposed low-complexity detectors in terms of visited nodes while still attaining the optimal BER performance of the maximum likelihood (ML) one. More recently, the authors in [25] introduced the first proposal of applying deep learning to detect data bits of the IM-OFDM systems. The proposed detector can provide a nearly optimal performance as the ML and reduces considerably the runtime of existing detectors.

In a recent work, a repeated index modulation-OFDM with coordinated interleaving (RIM-OFDM-CI) scheme was presented in [26]. In RIM-OFDM-CI, coordinate interleaving is simultaneously applied to the M-ary modulated symbols in two different clusters. Additionally, these distinct clusters repeatedly use the same set of active sub-carrier indices. Combining coordinate interleaving and the index repetition allows RIM-OFDM-CI to attain better index detection and the M-ary symbol error performance over the conventional IM-OFDM-CI system, even at the same spectral efficiency. Furthermore, while IM-OFDM-CI requires an even number of active sub-carriers, the proposed scheme can operate well with an arbitrary number of active sub-carriers and thus is more flexible in terms of achieving reliability and spectral efficiency.

The objective of this paper is to extend our work in [26] by conducting a detailed theoretical analysis on the performance of the RIM-OFDM-CI system. Based on this analysis, an optimal rotation angle for the signal constellation to optimize the system performance is determined. In addition, the efficient detectors to reduce the computational complexity are also proposed. The main contributions of the paper can be summarized as follows:

- We propose a repeated index modulation-OFDM with coordinate interleaving (RIM-OFDM-CI) which achieves better index and symbol error performance than IM-OFDM and IM-OFDM-CI. The proposed scheme is also more flexible in achieving the required transmission reliability and the spectral efficiency.
- The approximated expressions for SEP of the RIM-OFDM-CI system are derived for the case of the Rayleigh fading channel and perfect channel state information (CSI) at the receiver.
- An efficient solution to derive the optimal constellation rotation angle for performance optimization without using computer search is proposed.
- Two low-complexity detectors, called the log-likelihood ratio (LLR) and greedy (GD) detector, are proposed to facilitate the complexity requirement while still enjoying nearly optimal performance of the ML detector.
- Finally, various performance evaluations of the RIM-OFDM-CI system with the proposed solutions are conducted to validate the theoretical analysis and compare its performance with related benchmark systems.

The remainder of this paper is organized as follows. Section II describes the system model of the introduced RIM-OFDM-CI. Detailed performance analysis and optimization is presented in Section III. Section IV introduces the low-complexity detectors. Section V presents complexity estimation of the proposed detectors. Simulation results are reported in Section VI. Finally, the conclusion is given in Section VII.

Notation: Vectors and matrices are denoted by lower-case and upper-case bold letters; $C(\ ,\ )$ and $\lfloor\cdot\rfloor$ represent the binomial coefficient and the floor function, respectively. $\mathbb{E}\{\cdot\}$ is the expectation operation. $(\cdot)^R$ and $(\cdot)^I$ respectively denote the real and imaginary parts of a complex number. The moment generating function (MGF) notation is denoted by $\mathcal{M}(.)$.

II. System Model

The block diagram of RIM-OFDM-CI for a typical sub-block is depicted in Fig. 1. An N_t sub-carrier OFDM system is split into G sub-blocks of N_G sub-carriers, i.e., $N_t = GN_G$. Then, each sub-block is partitioned into two clusters. Each cluster has N sub-carriers, i.e., $N_G = 2N$. Since signal processing in each sub-block is similar and independent, without loss of generality, we will focus on a typical sub-block.

In each sub-block transmission, the incoming p data bits are divided into two bit sequences. The first $p_I = \lfloor \log_2 (C(N,K)) \rfloor$ bits are sent to an index mapper to determine K out of N sub-carriers for each clusters, where K is the number of active sub-carriers, using either a look-up table (LUT) or the combinatorial method [2]. Similar to the IM-OFDM system, additional data bits are transferred through the indices of active sub-carriers. The remaining $N-K$ sub-carriers are set to null. The output of the index mapper is a set of active sub-carrier indices $\theta = \{\alpha_1, \ldots, \alpha_K\}$, where α_k is the index of the k^{th} active sub-carrier with $\alpha_k \in \{1, \ldots, N\}$ for all $k \in \{1, 2, \ldots, K\}$. Let $\mathcal{I}$ denote the set of possible active indices. For given N and K, there are a total of $C = 2^{\lfloor \log_2 C(N,K) \rfloor}$ combinations of active indices. Unlike the IM-OFDM-CI system, RIM-OFDM-CI employs the same set of active indices θ for two clusters in one sub-block as shown in Fig. 1. The index repetition can improve the accuracy of the index detection compared to the conventional scheme at the cost of spectral efficiency.

The p_M bit sequence is equally separated into two clusters of $p_c = K\log_2 M$ bits, where M is the modulation order. By repeating the indices of sub-carriers, we can apply coordinate interleaving (CI) to the M-ary symbols of two clusters in a sub-block. In particular, for cluster i, $p_c = K\log_2 M$ bits are mapped into a vector of K complex data symbols $\mathbf{s}_i \in \mathbb{C}^{K\times 1}$, for $i = 1, 2$. Prior to coordinate interleaving, $\mathbf{s}_i$ is rotated by an angle ϕ which is properly designed to achieve the best performance for each M based on the performance analysis as shown later in Sect. III. The rotated constellation is denoted by $\mathcal{S}^\phi$. Let us denote $\mathbf{s}_1^\phi = [a_1\ a_2\ \ldots\ a_K]^T$ and $\mathbf{s}_2^\phi = [b_1\ b_2\ \ldots\ b_K]^T$, where $a_k, b_k \in \mathcal{S}^\phi$, $k \in \{1, 2, \ldots, K\}$. After coordinate interleaving between the symbols in $\mathbf{s}_1^\phi$ and $\mathbf{s}_2^\phi$ from different clusters, the symbol vectors in each cluster,

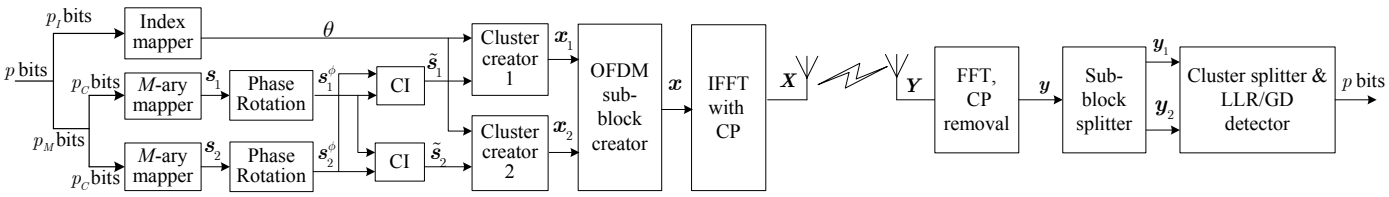

Fig. 1: Block diagram of a typical RIM-OFDM-CI sub-block.

$\tilde{\mathbf{s}}_i \in \mathbb{C}^{K\times 1}$, are obtained as follows:

$$\tilde{\mathbf{s}}_1 = \begin{bmatrix} c_{1,1} \\ c_{1,2} \\ \vdots \\ c_{1,K-1} \\ c_{1,K} \end{bmatrix} = \begin{bmatrix} a_1^R + jb_1^I \\ a_2^R + jb_2^I \\ \vdots \\ a_{K-1}^R + jb_{K-1}^I \\ a_K^R + jb_K^I \end{bmatrix} \tag{1}$$

$$\tilde{\mathbf{s}}_2 = \begin{bmatrix} c_{2,1} \\ c_{2,2} \\ \vdots \\ c_{2,K-1} \\ c_{2,K} \end{bmatrix} = \begin{bmatrix} b_1^R + ja_1^I \\ b_2^R + ja_2^I \\ \vdots \\ b_{K-1}^R + ja_{K-1}^I \\ b_K^R + ja_K^I \end{bmatrix}. \tag{2}$$

where $j = \sqrt{-1}$. Using $\tilde{\mathbf{s}}_i$ and θ, the transmitted codeword of cluster i, $\mathbf{x}_i = [x_{i1}, \ldots, x_{iN}]^T$, can be generated, where $x_{i\alpha_k} = c_{i,k}$ when $\alpha_k \in \theta$, and $x_{i\alpha} = 0$ when $\alpha \notin \theta$, and $\alpha_k \in \{1, \ldots, N\}$, $k \in \{1, \ldots, K\}$, $i = 1, 2$. An example of the transmitted codewords for $N = 4$, $K = 2$, $p_I = 2$ is presented in Table I. It can be seen from the proposed scheme that the real and imaginary parts of the original M-ary modulated symbols are transferred over different sub-carriers, leading to an improvement of the diversity gain. In addition, combining the index repetition and the joint coordinate interleaving allows RIM-OFDM-CI to activate an arbitrary number of sub-carriers which makes our scheme more flexible than the conventional IM-OFDM-CI.

The OFDM sub-block creator receives $\mathbf{x}_1$ and $\mathbf{x}_2$ to generate the transmitted vector per sub-block that is given by $\mathbf{x} = \left[\mathbf{x}_1^T \ \mathbf{x}_2^T\right]^T$. This transmit vector goes through the signal processing of the conventional OFDM transceiver including Inverse Fast Fourier Transform (IFFT) and cyclic-prefix (CP) addition in the transmitter, and CP removal and Fast Fourier Transform (FFT) at the receiver. Given that the CP is selected longer than the maximal channel delay, the frequency-selective fading channel is converted into multiple flat fading channels in each sub-band. Thus, under the assumption of the Rayleigh frequency selective fading channel, the coefficients of the sub-band channels can be modeled by Rayleigh distributed random variables with zero mean and variances $\sigma_{i\alpha}^2$. It is worth noting that $\sigma_{i\alpha}^2$ represents the sub-band channel gains which depend on the power delay profile of the channel. In this paper, to simplify mathematical analysis we assume that $\sigma_{i\alpha}^2 = 1$.

The received signal in the frequency domain can be then expressed as

$$\mathbf{y} = \mathbf{H}\mathbf{x} + \mathbf{n}, \tag{3}$$

where $\mathbf{y} = [\mathbf{y}_1 \ \mathbf{y}_2]^T$, $\mathbf{H} = \begin{bmatrix} \mathbf{H}_1 & \mathbf{0} \\ \mathbf{0} & \mathbf{H}_2 \end{bmatrix}$ and $\mathbf{n} = \left[\mathbf{n}_1^T \ \mathbf{n}_2^T\right]^T$. The components $\mathbf{y}_i = [y_{i1}, \ldots, y_{iN}]$ and $\mathbf{H}_i = \text{diag}\{h_{i1}, \ldots, h_{iN}\}$, for $i = 1, 2$, represent the received signal and channel matrix of cluster i, respectively. The noise component is given by $\mathbf{n}_i = [n_{i1}, \ldots, n_{iN}]^T$. The channel coefficient and noise on each sub-carrier follow the distributions $h_{i\alpha} \sim \mathcal{CN}(0, 1)$ and $n_{i\alpha} \sim \mathcal{CN}(0, N_0)$, where N_0 represents the noise variance. Let us define the average signal to noise ratio (SNR) per sub-carrier by $\bar{\gamma} = \omega E_s / N_0$, where ωE_s denotes the average transmit power per an M-ary modulated symbol, $\mathbb{E}\{|s|^2\} = \omega E_s$. The power allocation factor and the average power per sub-carrier are denoted by $\omega = N/K$ and E_s, respectively.

Therefore, the number of transmitted bits in each sub-block is given by $p = p_I + p_M$ bits, which results in the spectral efficiency, measured in bits/s/Hz, as follows:

$$\eta = \frac{\lfloor \log_2 \left(C\left(N, K\right)\right) \rfloor + 2K \log_2 M}{2N}. \tag{4}$$

It can be seen that the spectral efficiency of the proposed system is lower than that of the conventional IM-OFDM [2] and IM-OFDM-CI [14] system. This is a drawback of the proposed system in comparison with the IM-OFDM system without repeated transmission.

To detect the transmitted signal, the receiver employs an ML detector to jointly estimate the active indices and the corresponding data symbols for both clusters as follows

$$\left(\hat{\theta}, \hat{\mathbf{s}}_1, \hat{\mathbf{s}}_2\right) = \arg \min_{\theta, \mathbf{s}_1, \mathbf{s}_2} \|\mathbf{y} - \mathbf{H}\mathbf{x}\|_F^2. \tag{5}$$

It can be seen that the complexity of the ML detector is $\mathcal{O}\left(2^{p_1} M^{2K}\right)$ which exponentially increases with M. For practical implementations, we propose two low-complexity detectors in the later section.

III. Performance Analysis

A. Symbol Error Probability Derivation

In this section, the error performance of the RIM-OFDM-CI system under the Rayleigh fading channel is analyzed via the symbol error probability (SEP). SEP is defined as the

TABLE I: Example of LUT for $N = 4$, $K = 2$, $p_1 = 2$.

p_I	θ	$\mathbf{x}_1^T$	$\mathbf{x}_2^T$
00	$[1, 2]$	$[a_1^R + jb_1^I \quad a_2^R + jb_2^I \quad 0 \quad 0]$	$[b_1^R + ja_1^I \quad b_2^R + ja_2^I \quad 0 \quad 0]$
01	$[2, 3]$	$[0 \quad a_1^R + jb_1^I \quad a_2^R + jb_2^I \quad 0]$	$[0 \quad b_1^R + ja_1^I \quad b_2^R + ja_2^I \quad 0]$
10	$[2, 4]$	$[0 \quad a_1^R + jb_1^I \quad 0 \quad a_2^R + jb_2^I]$	$[0 \quad b_1^R + ja_1^I \quad 0 \quad b_2^R + ja_2^I]$
11	$[1, 3]$	$[a_1^R + jb_1^I \quad 0 \quad a_2^R + jb_2^I \quad 0]$	$[b_1^R + ja_1^I \quad 0 \quad b_2^R + ja_2^I \quad 0]$

ratio of the total number of possible symbols in error to the total number of transmit symbols consisting of index and M-ary symbols, which can be mathematically expressed as follows [10]:

$$P_s = \frac{P_I + KP_M}{K+1}, \tag{6}$$

where P_I and P_M are the index and M-ary symbol error probabilities, respectively. In order to determine SEP, it is necessary to firstly determine P_M. Following the frame work in [27], the average SEP for M-ary symbols of the RIM-OFDM-CI system is given by

$$P_M = \frac{1}{|\mathcal{S}^\phi|} \sum_{a_1 \in \mathcal{S}^\phi} \sum_{\hat{a}_1 \neq a_1} \mathbb{E}\left\{Q\left(\sqrt{\Omega}\right)\right\}, \tag{7}$$

where $\Omega = \frac{\gamma_1 \Delta_R^2 + \gamma_2 \Delta_I^2}{2}$ and $\Delta_R^2 = |a_1^R - \hat{a}_1^R|^2$; $\Delta_I^2 = |a_1^I - \hat{a}_1^I|^2$. Based on the approximation of Q-function [28], $Q(\Omega)$ can be approximated as follows:

$$Q\left(\sqrt{\Omega}\right) \approx \frac{1}{12} e^{-\frac{\Omega}{2}} + \frac{1}{4} e^{-\frac{2\Omega}{3}}, \tag{8}$$

Then, applying the moment generating function (MGF) for the Rayleigh fading channel [29] $\mathcal{M}_\gamma(t) = (1 - \overline{\gamma} t)^{-1}$, the MGF of Ω is given by

$$\mathcal{M}_\Omega(t) = \frac{1}{\left(1 - \frac{\bar{\gamma}\Delta_R^2 t}{2}\right)\left(1 - \frac{\bar{\gamma}\Delta_I^2 t}{2}\right)}. \tag{9}$$

Using the MGF approach, the approximated SEP for M-ary modulated symbols of the RIM-OFDM-CI system is calculated by

$$\begin{aligned} P_M &\approx \frac{\mathcal{M}_\Omega\left(-\frac{1}{2}\right)}{12} + \frac{\mathcal{M}_\Omega\left(-\frac{2}{3}\right)}{4} \\ &\approx \frac{1}{12\left(1 + \frac{\bar{\gamma}\Delta_R^2}{4}\right)\left(1 + \frac{\bar{\gamma}\Delta_I^2}{4}\right)} + \frac{1}{4\left(1 + \frac{\bar{\gamma}\Delta_R^2}{3}\right)\left(1 + \frac{\bar{\gamma}\Delta_I^2}{3}\right)}. \end{aligned} \tag{10}$$

Since different clusters in the RIM-OFDM-CI system use the same set of active sub-carrier indices, this index repetition can improve the accuracy of index detection.

Consequently, the average SEP of the RIM-OFDM-CI system is approximated by

$$P_s \approx \Psi \left[\frac{1}{12\left(1 + \frac{\bar{\gamma}\Delta_R^2}{4}\right)\left(1 + \frac{\bar{\gamma}\Delta_I^2}{4}\right)} + \frac{1}{4\left(1 + \frac{\bar{\gamma}\Delta_R^2}{3}\right)\left(1 + \frac{\bar{\gamma}\Delta_I^2}{3}\right)} \right], \tag{11}$$

where $\Psi = K/(K+1)$.

At high SNR, the average SEP in (11) is approximated by

$$P_s \approx \frac{43K^3}{12N^2(K+1)} \frac{1}{\Delta_R^2 \Delta_I^2} \frac{1}{{\gamma_0}^2} \approx \Theta\left(\left(c_g \gamma_0\right)^{-2}\right), \tag{12}$$

where coding gain c_g is given by

$$c_g = \frac{N}{K\sqrt{\frac{43K}{12(K+1)} \frac{1}{\Delta_R^2 \Delta_I^2}}} \tag{13}$$

Remark 1: As can be seen from (12) that RIM-OFDM-CI attains diversity order of 2. At high SNRs, for a given K, the SEP of RIM-OFDM-CI is strongly influenced by the product $\Delta_I^2 \Delta_R^2$. The best SEP is achieved by minimizing the value of $1/\Delta$, where $\Delta = \Delta_I^2 \Delta_R^2$. For the given M, Δ is affected by the rotation angle ϕ. This motivates us to determine an optimal rotation angle to minimize the error performance.

Remark 3: Based on the framework in [12], the average BER of RIM-OFDM-CI can be approximated by

$$P_b \approx \Gamma \left[\frac{1}{12\left(1 + \frac{\bar{\gamma}\Delta_R^2}{4}\right)\left(1 + \frac{\bar{\gamma}\Delta_I^2}{4}\right)} + \frac{1}{4\left(1 + \frac{\bar{\gamma}\Delta_R^2}{3}\right)\left(1 + \frac{\bar{\gamma}\Delta_I^2}{3}\right)} \right], \tag{14}$$

where $\Gamma = K/(p_I + p_c)$

B. Optimization of Rotation Angle

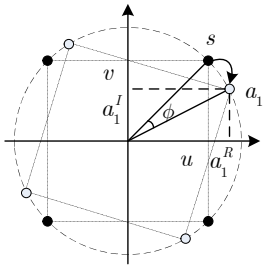

Fig. 2: Rotated signal constellation for 4-QAM.

In this section, without utilizing computer search, a solution to determine the optimal rotation angle, denoted by ϕ_{opt}, to minimize SEP based on the above performance analysis is introduced. For simplicity, we only analyze in detail the case of quadrature amplitude modulation (QAM) constellation with

$M = 4$ as shown in Fig. 2. Following this figure, the imaginary and real parts of the data symbol after phase rotation can be represented by

$$\begin{aligned} a_1^R &= u\cos\phi + v\sin\phi, \\ a_1^I &= -u\sin\phi + v\cos\phi. \end{aligned} \tag{15}$$

Besides, following performance analysis, the minimization of SEP becomes the minimization of the value of J function given by

$$J = \sum_{\hat{a}_1 \neq a_1} P\left(a_1 \to \hat{a}_1\right). \tag{16}$$

According to asymptotic analysis and using (15), $P\left(a_1 \to \hat{a}_1\right)$ can be rewritten as

$$P\left(a_1 \to \hat{a}_1\right) \leq P_1 P_2, \tag{17}$$

where P_1, P_2 are respectively given by

$$\begin{aligned} P_1 &= \frac{1}{1 + \bar{\gamma}\left|\left(u - \hat{u}\right)\cos\phi + \left(v - \hat{v}\right)\sin\phi\right|^2}, \\ P_2 &= \frac{1}{1 + \bar{\gamma}\left|-\left(u - \hat{u}\right)\sin\phi + \left(v - \hat{v}\right)\cos\phi\right|^2}. \end{aligned} \tag{18}$$

It can be seen that $\phi = 0$ leading to $a_1^R = u$, $a_1^I = v$, then P_1 and P_2 become

$$P_1 = \frac{1}{1 + \bar{\gamma}\left|\left(u - \hat{u}\right)\right|^2}; P_2 = \frac{1}{1 + \bar{\gamma}\left|\left(v - \hat{v}\right)\right|^2}. \tag{19}$$

As observed from (18) and (19) that the value of ϕ strongly decides to the error performance. It motivates us to determine ϕ_{opt} such that the error performance is minimum. At the high SNR regime, J can be approximated as

$$J \approx \left(\frac{2}{\sin^2 2\phi} + \frac{1}{4\cos^2 2\phi}\right)\frac{1}{\bar{\gamma}^2}. \tag{20}$$

After some straight mathematical manipulations, we can calculate the optimum rotation angle for 4-PSK scheme $\phi_{\text{opt}} = 30^\circ$. Applying the similar process, we can determine the following optimum values: $\phi_{\text{opt}} = \{45^\circ, 30^\circ, 9.5^\circ, 40^\circ\}$ for $M = \{2, 4, 8, 16\}$, respectively. Note that for $M = 2$ and $M = 8$, the phase shift keying (PSK) is used instead of QAM.

IV. Low-Complexity Detectors for RIM-OFDM-CI

In this section, two low-complexity detectors that can achieve the optimum and near-optimum performance of the ML detector, called LLR and GD detection, are proposed. The detection process is divided into two steps: the first step is to detect the indices of active sub-carriers. Based on detected indices, the data symbols corresponding to active sub-carriers are recovered in the second step.

1) LLR detector: In order to estimate the indices of active sub-carriers, the LLR detector calculates the following LLR for each sub-carrier [16]

$$\lambda\left(\alpha\right) = \left|y_{1\alpha}\right|^2 - \left|y_{1\alpha} - h_{1\alpha}s_m\right|^2 + \left|y_{2\alpha}\right|^2 - \left|y_{2\alpha} - h_{2\alpha}s_m\right|^2, \tag{21}$$

where $\alpha = 1, \ldots, N$, $m = 1, \ldots, M$, $s_m \in \mathcal{S}^\phi$. Based on N computed LLR values, the LLR detector selects the K largest LLR values to determine the set of active sub-carrier indices.

Upon detecting the indices of active sub-carriers, the corresponding data symbols can be estimated. For each active sub-carrier set $\hat{\theta} = \{\hat{\alpha}_1, \ldots, \hat{\alpha}_K\}$, we can express the received signal for active sub-carrier $\hat{\alpha}_k \in \hat{\theta}$, $k = 1, ..., K$ as follows

$$\begin{aligned} \begin{bmatrix} y_{1\hat{\alpha}_k}^R \\ y_{1\hat{\alpha}_k}^I \\ y_{2\hat{\alpha}_k}^R \\ y_{2\hat{\alpha}_k}^I \end{bmatrix} &= \begin{bmatrix} h_{1\hat{\alpha}_k}^R & 0 & 0 & -h_{1\hat{\alpha}_k}^I \\ h_{1\hat{\alpha}_k}^I & 0 & 0 & h_{1\hat{\alpha}_k}^R \\ 0 & -h_{2\hat{\alpha}_k}^I & h_{2\hat{\alpha}_k}^R & 0 \\ 0 & h_{2\hat{\alpha}_k}^R & h_{2\hat{\alpha}_k}^I & 0 \end{bmatrix} \\ &\times \begin{bmatrix} a_k^R \\ a_k^I \\ b_k^R \\ b_k^I \end{bmatrix} + \begin{bmatrix} n_{1\hat{\alpha}_k}^R \\ n_{1\hat{\alpha}_k}^I \\ n_{2\hat{\alpha}_k}^R \\ n_{2\hat{\alpha}_k}^I \end{bmatrix} \end{aligned} \tag{22}$$

Equation (22) can be rewritten in the vector form as follows

$$\bar{\mathbf{y}}_{\hat{\alpha}_k} = \bar{\mathbf{H}}_{\hat{\alpha}_k}\bar{\mathbf{s}}_k + \bar{\mathbf{n}}_{\hat{\alpha}_k}, \tag{23}$$

where $\bar{\mathbf{H}}_{\hat{\alpha}_k} = \left[\bar{\mathbf{H}}_{1\hat{\alpha}_k}\ \bar{\mathbf{H}}_{2\hat{\alpha}_k}\right]^T$, and $\bar{\mathbf{H}}_{1\hat{\alpha}_k}$, $\bar{\mathbf{H}}_{2\hat{\alpha}_k}$ are respectively given by

$$\bar{\mathbf{H}}_{1\alpha_k} = \begin{bmatrix} h_{1\hat{\alpha}_k}^R & 0 \\ h_{1\hat{\alpha}_k}^I & 0 \\ 0 & -h_{2\hat{\alpha}_k}^I \\ 0 & h_{2\hat{\alpha}_k}^R \end{bmatrix}, \quad \bar{\mathbf{H}}_{2\hat{\alpha}_k} = \begin{bmatrix} 0 & -h_{1\hat{\alpha}_k}^I \\ 0 & h_{1\hat{\alpha}_k}^R \\ h_{2\hat{\alpha}_k}^R & 0 \\ h_{2\hat{\alpha}_k}^I & 0 \end{bmatrix}. \tag{24}$$

Since columns of channel matrix $\bar{\mathbf{H}}_{\hat{\alpha}_k}$ are orthogonal, data symbols $\hat{a}_k$ and $\hat{b}_k$ can be detected independently by the single-symbol ML detector as follows

$$\begin{aligned} \hat{a}_k &= \arg\min_{a_k \in \mathcal{S}^\phi} \left\| \bar{\mathbf{y}}_{\hat{\alpha}_k} - \bar{\mathbf{H}}_{1\hat{\alpha}_k}\left[a_k^R\ a_k^I\right]^T \right\|_F^2, \\ \hat{b}_k &= \arg\min_{b_k \in \mathcal{S}^\phi} \left\| \bar{\mathbf{y}}_{\hat{\alpha}_k} - \bar{\mathbf{H}}_{2\hat{\alpha}_k}\left[b_k^R\ b_k^I\right]^T \right\|_F^2. \end{aligned} \tag{25}$$

Based on estimated symbols $\hat{a}_k$ and $\hat{b}_k$, $k = 1, \ldots, K$, the symbol vectors for each cluster is recovered as

$$\begin{aligned} \hat{\mathbf{s}}_1 &= \left[\hat{a}_1\ \hat{a}_2\ \ldots\ \hat{a}_K\right]^T, \\ \hat{\mathbf{s}}_2 &= \left[\hat{b}_1\ \hat{b}_2\ \ldots\ \hat{b}_K\right]^T. \end{aligned} \tag{26}$$

2) GD detector: Compared to LLR, GD detector differs only in estimating the active sub-carrier set. The GD detector estimates the K indices of active sub-carriers based on K out of N sub-carriers which have the highest power sum of the two groups, i.e, $\left|y_1\left(\alpha\right)\right|^2 + \left|y_2\left(\alpha\right)\right|^2$. The estimation of the corresponding M-ary symbols is similar to that by the LLR detector. Although the GD detection does not work well with

IM-OFDM-CI and ReMO system, it effectively supports the proposed RIM-OFDM-CI.

The LLR and GD detection algorithms are summarized in Algorithm 1 and Algorithm 2, respectively.

Algorithm 1 LLR Detection Algorithm

Input: $\mathbf{y}_1$, $\mathbf{y}_2$, $\mathbf{H}_1$, $\mathbf{H}_2$, $\mathcal{S}^{\phi}$, $\mathcal{I}$.
Output: $\hat{\theta}$, $\hat{\mathbf{s}}_1$, $\hat{\mathbf{s}}_2$.
1: Compute N LLR values $\lambda(\alpha)$ according to (21).
2: Find K largest LLR values to estimate $\hat{\theta}$.
3: **for** $k = 1$ **to** K **do**
4: Define $\bar{\mathbf{y}}_{\hat{\alpha}_k} = \left[y^R_{1\hat{\alpha}_k}\ y^I_{1\hat{\alpha}_k}\ y^R_{2\hat{\alpha}_k}\ y^I_{2\hat{\alpha}_k}\right]^T$.
5: Compute $\bar{\mathbf{H}}_{1\hat{\alpha}_k}$, $\bar{\mathbf{H}}_{2\hat{\alpha}_k}$ according to (24).
6: Estimate $\hat{a}_k$ and $\hat{b}_k$ according to (25).
7: **end for**
8: Generate $\hat{\mathbf{s}}_1$, $\hat{\mathbf{s}}_2$ according to (26).
9: Output: $\hat{\theta}$, $\hat{\mathbf{s}}_1$, $\hat{\mathbf{s}}_2$.

Algorithm 2 GD Detection Algorithm

Input: $\mathbf{y}_1$, $\mathbf{y}_2$, $\mathbf{H}_1$, $\mathbf{H}_2$, $\mathcal{S}^{\phi}$, $\mathcal{I}$.
Output: $\hat{\theta}$, $\hat{\mathbf{s}}_1$, $\hat{\mathbf{s}}_2$.
1: Calculate N values of $\Xi(\alpha)$:
2: $\Xi(\alpha) = |y_1(\alpha)|^2 + |y_2(\alpha)|^2$, for $\alpha = 1, \ldots, N$.
3: Find K highest values of $\Xi(\alpha)$ to detect $\hat{\theta}$
4: **for** $k = 1$ **to** K **do**
5: Define $\bar{\mathbf{y}}_{\hat{\alpha}_k} = \left[y^R_{1\hat{\alpha}_k}\ y^I_{1\hat{\alpha}_k}\ y^R_{2\hat{\alpha}_k}\ y^I_{2\hat{\alpha}_k}\right]^T$.
6: Compute $\bar{\mathbf{H}}_{1\hat{\alpha}_k}$, $\bar{\mathbf{H}}_{2\hat{\alpha}_k}$ according to (24).
7: Estimate $\hat{a}_k$ and $\hat{b}_k$ according to (25).
8: **end for**
9: Generate $\hat{\mathbf{s}}_1$, $\hat{\mathbf{s}}_2$ according to (26).
10: Output: $\hat{\theta}$, $\hat{\mathbf{s}}_1$, $\hat{\mathbf{s}}_2$.

V. Complexity Analysis

This section evaluates the computational complexity of the proposed detectors in comparison with the ML and LowML detectors. The complexity of the considered detectors are expressed by the number of floating points (flops) per sub-carriers. Assume that a real summation, real subtraction or a real multiplication is presented by a flop. A complex summation and a complex multiplication account for 2 and 6 flops, respectively. For the LLR detector, it requires $26M + 7$ flops per sub-carrier for calculating value of $\lambda(\alpha)$. There is a total of N values of α, thus requiring $26MN + 7N$ flops to calculate N LLR values. Unlike the LLR detector, the GD detects active sub-carrier indices based on the power sum of the two groups, which requires $10N$ flops. Based on equation (25), the detection of M-ary modulated symbols of the two detectors is similar, which requires $94MK$ flops.

The ML detector searches exhaustedly for all active sub-carrier index combinations and corresponding data symbols to jointly detect them. Based on equation (5), the complexity of ML detector is given by $(30N - 2)\,CM^{2K}$ where $30N - 2$ is number flops per trial, $C = 2^{\lfloor \log_2 C(N,K) \rfloor}$ is the total number of combinations of the active sub-carrier indices. Using the similar estimation for LowML, the computational complexities of RIM-OFDM-CI using various detectors are estimated and summarized in Table II.

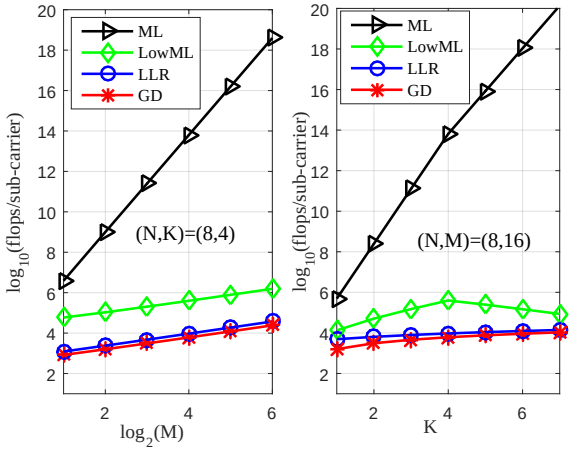

Fig. 3: Computational complexity of proposed detectors in comparison with ML and LowML detectors.

As can be seen from Table II that the ML detector has the highest complexity in terms of number of flops per sub-carrier, which grows exponentially with M, while those of the LowML, GD and LLR detectors are linearly proportional to M. In spite of having the same detection process, the GD detector still can reduce the computational complexity in comparison with the LLR detector. In particular, when the values of N, K, M are small, such as $(N, K, M) = (4, 2, 4)$, the LLR detector saves 84.16 % and 64.23 % of computational complexity compared to the ML and the LowML detectors, respectively. Meanwhile the complexity savings of the GD detector compared to two benchmark detectors are up to nearly 90.51 % and 76.32 %, respectively. Interestingly, for large N, K, M, for example $(N, K, M) = (8, 4, 8)$, the LLR and the GD detector reduce complexities of the ML by 99.58 %, 99.68 % and that of LowML by 97.68 %, 98.48 %. It can be seen that the complexity of the LLR detector is close to that of the GD when N, K, M are high. This statement is validated by numerical results in Fig. 3.

VI. Performance Evaluations and Discussions

This section presents performance evaluations of the proposed RIM-OFDM-CI scheme and low-complexity detectors using analytical and simulation results. Assume that the channel over each sub-carrier is flat Rayleigh fading. For comparison, IM-OFDM [2], IM-OFDM-CI [14] and ReMO [21] using ML, LLR and GD detectors are chosen as benchmarks. It is worth noting that the GD detector does not help the IM-OFDM-CI and ReMO schemes to improve the system performance while it can work effectively with the proposed RIM-CI-OFDM system. Interestingly, RIM-OFDM-CI using

TABLE II: Complexity comparison between ML, LowML, LLR and GD dectectors.

Detector	***Number of flops***	***Order of complexity***	$(N,K,M)=(4,2,4)$	$(N,K,M)=(8,4,8)$
ML	$(30N-2)\,CM^{2K}$	$\mathcal{O}\left(NCM^{2K}\right)$	7,552	974,848
LowML	$(2K+20N+94MK)\,C$	$\mathcal{O}\left(MCK\right)$	3,344	203,264
LLR	$26MN+7N+94MK$	$\mathcal{O}\left(NM\right)$	1,196	4,728
GD	$10N+94MK$	$\mathcal{O}\left(N\right)$	792	3,088

the LLR detector can achieve considerably better performance than RIM-OFDM-CI with the GD detector at the equivalent complexity when (N,K,M) are large. For simplicity, system configuration with K out of N active sub-carriers and modulation order M is referred to as (N,K,M).

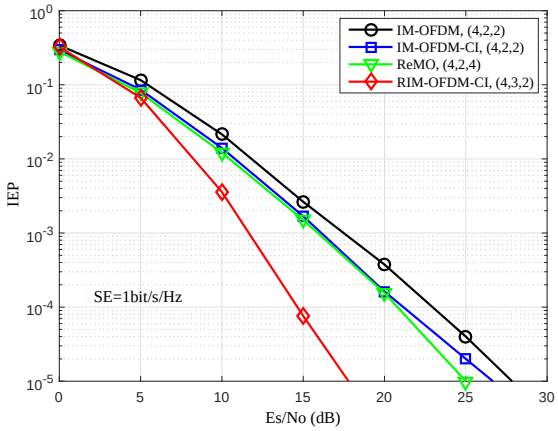

Fig. 4: Index error performance of RIM-OFDM-CI, IM-OFDM, IM-OFDM-CI and ReMO systems at the spectral efficiency of 1 bit/s/Hz, $M=\{2,4\}$, $N=4$, $K=\{2,3\}$.

Fig. 4 compares the index error probability (IEP) of the proposed RIM-OFDM-CI, the conventional IM-OFDM, IM-OFDM-CI and ReMO systems at the same spectral efficiency of 1 bit/s/Hz when $M=\{2,4\}$, $N=4$, $K=\{2,3\}$. Note that in this figure and the following ones, in addition to guarantee the same spectral efficiency, we chose $K=3$ in our proposed scheme to prove that it can operate well with an odd number of K. It can be seen from the figure that the proposed scheme has significantly improved IEP performance over the reference systems. Particularly, at IEP of 10^{-4}, it attains SNR gains of about 8 dB and 5.5 dB over the IM-OFDM and IM-OFDM-CI/ReMO systems, respectively. Since the proposed scheme employs joint index repetition and coordinate interleaving, it can achieve better diversity gain in the index domain than the benchmarks.

The spectral efficiency of RIM-OFDM-CI compared to the benchmark systems is shown in Fig. 5. The curve for RIM-OFDM-CI was plotted using equation (4), that for IM-OFDM using [2], IM-OFDM-CI using [14], and ReMO using [21]. It is observed that the spectral efficiency of the proposed system is lower than that of the conventional IM-OFDM and IM-OFDM-CI systems at all K but higher than that of ReMO for $K>2$.

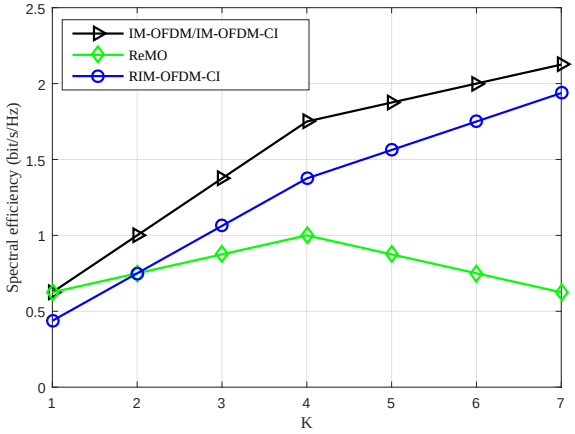

Fig. 5: The spectral efficiency of the RIM-OFDM-CI system in comparison with that of the IM-OFDM, IM-OFDM-CI and ReMO systems when $N=8$, $M=4$ and $K=\{1,2,\ldots,7\}$.

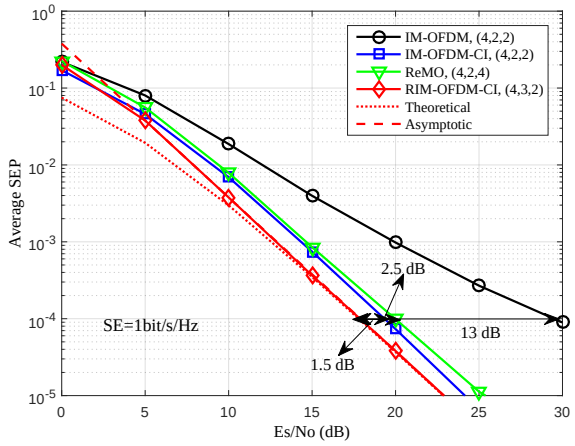

Fig. 6: SEP comparison between RIM-OFDM-CI, IM-OFDM and IM-OFDM-CI using ML detection at the spectral efficiency of 1 bit/s/Hz when $M=\{2,4\}$, $N=4$, $K=\{2,3\}$.

Fig. 6 depicts the SEP performance comparison between RIM-OFDM-CI, IM-OFDM, IM-OFDM-CI and ReMO systems at the same spectral efficiency of 1 bit/s/Hz for $M=$

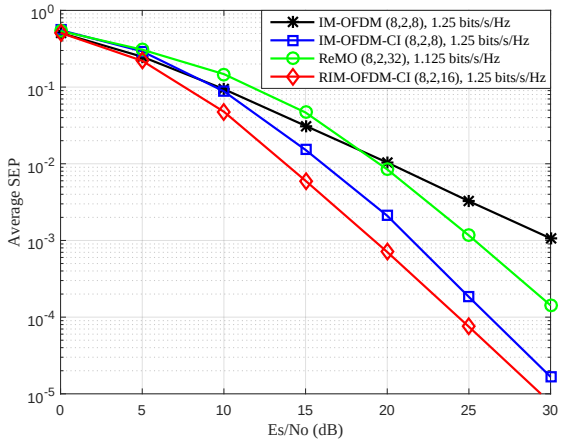

Fig. 7: SEP comparison between RIM-OFDM-CI, IM-OFDM, IM-OFDM-CI and ReMO using ML detection at the similar spectral efficiency for $N = 4$, $K = 2$ and appropriate M.

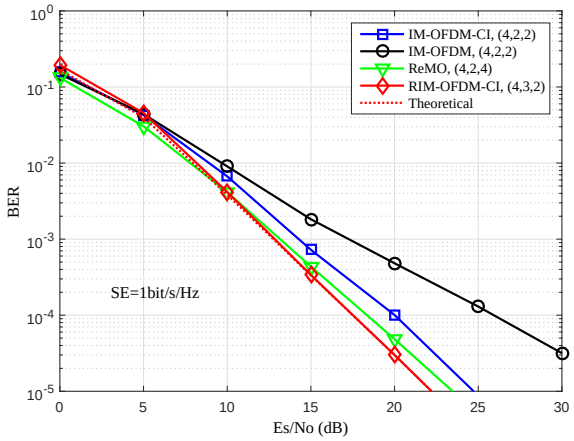

Fig. 8: BER comparison between the proposed scheme and the benchmarks when $N = 4$, $K = \{2, 3\}$, $M = \{2, 4\}$.

$\{2, 4\}$, $N = 4$, $K = \{2, 3\}$. The ML detector is employed in all considered schemes. As can be seen that at the same spectral efficiency and SEP of 10^{-4}, the proposed scheme provides SNR gain of about 13 dB, 1.5 dB and 2.5 dB over the IM-OFDM, IM-OFDM-CI and ReMO, respectively. This achieved gain is thanks to the improved IEP performance. As clearly shown in Fig. 4, improvement in the IEP performance helps to reduce the data symbol errors, leading to the better overall error performance compared to the benchmarks.

Fig. 7 illustrates the average SEP performance comparison between the proposed scheme and the benchmark systems. In this figure, the spectral efficiency is set to 1.25 bits/s/Hz for IM-OFDM, IM-OFDM-CI and RIM-OFDM-CI, and 1.125 bits/s/Hz for ReMO. All schemes use the same $N = 8$ and $K = 2$ while M is chosen appropriately for the above spectral efficiencies. Specifically, $M = 8$ for IM-OFDM, IM-OFDM-CI, $M = 32$ for ReMO and $M = 16$ for RIM-OFDM-CI. It is observed that at the same subcarrier setting, i.e. the same N and K, and similar spectral efficiency, the proposed RIM-OFDM-CI scheme still attains better SEP performance than the benchmark systems.

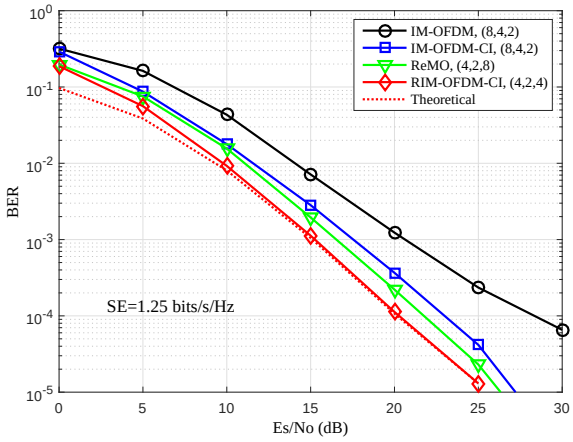

Fig. 9: BER comparison between the proposed and benchmarks at spectral efficiency of 1.25 bits/s/Hz when $N = \{4, 8\}$, $K = \{2, 4\}$, $M = \{2, 4, 8\}$.

The BER comparison between the proposed scheme, IM-OFDM, IM-OFDM-CI and ReMO when $N = 4$, $K = \{2, 3\}$, $M = \{2, 4\}$ is shown in Fig. 8. All considered schemes use the same ML detection. As clearly shown in the figure, at the same spectral efficiency of 1 bit/s/Hz, the proposed scheme achieves better BER performance than the benchmark systems. For example, at $\text{BER} = 10^{-4}$, the proposed scheme can obtain SNR gains of 9 dB, 2.5 dB and 0.5 dB over IM-OFDM, IM-OFDM-CI and ReMO, respectively.

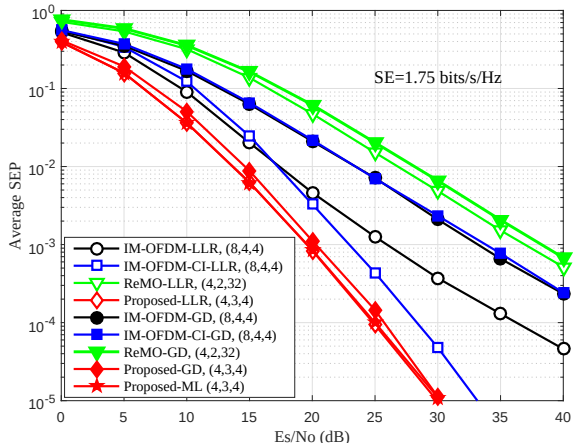

Fig. 10: SEP performance of RIM-OFDM-CI and benchmark systems using different detectors.Fig10

BER performance of the proposed scheme in comparison

with the benchmarks at higher spectral efficiency is shown in Fig. 9. At the spectral efficiency of 1.25 bits/s/Hz, RIM-OFDM-CI still outperforms the benchmark systems. Specifically, at the BER of 10^{-4}, the proposed scheme can provide the SNR gains of nearly 9 dB, 3 dB and 1.5 dB over the conventional IM-OFDM, IM-OFDM-CI and ReMO, respectively. Also noted from Fig. 5, Fig. 6 and Fig. 7 that at the high SNR region, the theoretical and simulated curves of both SEP and BER of the proposed scheme coincide for all investigated configurations, such as $(N, K, M) = (4, 3, 2)$ and $(N, K, M) = (4, 2, 4)$. This validates the accuracy of the analytical expression for SEP and BER of the proposed scheme in (11) and (14).

For comparison of energy efficiency between RIM-OFDM-CI and the benchmark schemes, we can use the method for estimating the required SNR per a reliable transmission bit in [9]. In order to achieve a quantitative comparison of energy efficiency in terms of bits/Joule/N_0, this method requires extensive computer simulations to estimate the spectral efficiency versus SNR. In contrast, for qualitative comparison, we can use the BER curves to compare the required SNR or E_s/N_0 to achieve the same BER. From Figs. 8 and 9, it can be seen that the proposed RIM-OFDM-CI scheme achieves better BER performance over the benchmark systems. Considering BERs smaller than 10^{-2}, which are often required in wireless communication systems, we can see that the proposed scheme requires less E_s/N_0 compared to all benchmark ones. This means that the proposed scheme is more efficient in terms of energy efficiency. However, it is worth noting that the BER improvement of the proposed scheme can only be achieved for low-rate, i.e. spectral efficiency smaller than 1.75 bps/Hz, systems when ML detector is used. For this reason, the proposed RIM-OFDM system is more suitable for communication systems which do not require very high transmission rate spectral efficiency, but more reliability such as Internet of Things, machine type communication (MTC) systems.

The SEP performance of RIM-OFDM-CI and the reference systems using the ML, LLR, GD detectors at the same spectral efficiency of 1.75 bits/s/Hz when $M = \{4, 32\}$, $N = \{4, 8\}$, $K = \{2, 3, 4\}$ are compared in Fig. 10. It can be seen that the conventional IM-OFDM-CI and ReMO systems do not perform well with the LLR and GD detectors, especially GD detector. Meanwhile, the proposed system with GD can provide better error performance than that of benchmark systems. Since the proposed system uses index repetition, it attains significant improvement in the index detection performance. Thus, the index detection in the first process of GD and LLR is more reliable. It can be observed from Fig. 10 that the proposed scheme using LLR detector significantly outperforms the IM-OFDM-LLR, IM-OFDM-CI-LLR and ReMO-LLR. Particularly, at the same spectral efficiency of 1.75 bits/s/Hz and the SEP of 10^{-3}, RIM-OFDM-CI-LLR provides a gain of about 6 dB, 3.5 dB and 17 dB over IM-OFDM, IM-OFDM-CI and ReMO using LLR detector, respectively. When using LLR, the proposed scheme also attains the same performance of the ML detector, while having much lower complexity compared to ML. Following the Fig. 10, we can see that the proposed system aided GD detection also considerably improves error performance of the benchmark systems utilizing GD. In particular, when using GD detector, at the SEP of 10^{-3}, the proposed scheme obtains the SNR gain of around 13 dB over the conventional IM-OFDM and IM-OFDM-CI systems and 19 dB over the ReMO scheme.

VII. Conclusion

This paper has analyzed error performance of the repeated IM-OFDM with coordinate interleaving and proposed two low-complexity detectors. The proposed system using two proposed LLR and GD detectors achieved better error performance than that of the conventional IM-OFDM-CI with LLR and GD ones. By applying the same set of active sub-carrier indices in two distinguishable clusters and employing coordinate interleaving for M-ary modulated symbols, the proposed RIM-OFDM-CI scheme can improve both the index and symbol error performances. Thus, the proposed system provides higher transmission reliability and attain the more flexible trade-off between the error performance than the conventional IM-OFDM-CI system. The derived analytical expressions provide a helpful insight into the influence of the system parameters on the error performance. Taking this advantage, the optimum constellation rotation angle is determined to minimize the error probability of the proposed scheme. Furthermore, two proposed low-complexity detectors allow the system to reduce detection complexity while enjoying comparable SEP performance with the ML detector. The analytical and simulation results clearly confirmed the advantages of the proposed scheme over the benchmark systems, especially when using the low-complexity detectors.

References

[1] R. Abu-Alhiga and H. Haas, "Subcarrier-index modulation OFDM," in *IEEE Int. Sym. Pers., Indoor and Mobile Radio Commun.* IEEE, Sep. 2009, pp. 177–181.

[2] E. Başar, Ü. Aygölü, E. Panayırcı, and H. V. Poor, "Orthogonal frequency division multiplexing with index modulation," *IEEE Trans. Signal Process.*, vol. 61, no. 22, pp. 5536–5549, Aug. 2013.

[3] Y. Xiao, S. Wang, L. Dan, X. Lei, P. Yang, and W. Xiang, "OFDM with interleaved subcarrier-index modulation," *IEEE Commun. Lett.*, vol. 18, no. 8, pp. 1447–1450, Jun. 2014.

[4] M. Wen, X. Cheng, M. Ma, B. Jiao, and H. V. Poor, "On the achievable rate of OFDM with index modulation," *IEEE Trans. Signal Process.*, vol. 64, no. 8, pp. 1919–1932, Apr. 2016.

[5] B. Zheng, F. Chen, M. Wen, F. Ji, H. Yu, and Y. Liu, "Low-complexity ML detector and performance analysis for OFDM with in-phase/quadrature index modulation," *IEEE Commun. Lett*, vol. 19, no. 11, pp. 1893–1896, Nov. 2015.

[6] T. Mao, Z. Wang, Q. Wang, S. Chen, and L. Hanzo, "Dual-mode index modulation aided OFDM," *IEEE Access*, vol. 5, pp. 50–60, Feb. 2017.

[7] M. Wen, E. Basar, Q. Li, B. Zheng, and M. Zhang, "Multiple-mode orthogonal frequency division multiplexing with index modulation," *IEEE Trans. Commun.*, vol. 65, no. 9, pp. 3892–3906, May. 2017.

[8] M. Wen, B. Ye, E. Basar, Q. Li, and F. Ji, "Enhanced orthogonal frequency division multiplexing with index modulation," *IEEE Trans. Wireless Commun.*, vol. 16, no. 7, pp. 4786–4801, May. 2017.

[9] H. Zhang, L.-L. Yang, and L. Hanzo, "Compressed sensing improves the performance of subcarrier index-modulation-assisted OFDM," *IEEE Access*, vol. 4, pp. 7859–7873, Oct. 2016.

[10] Y. Ko, "A tight upper bound on bit error rate of joint OFDM and multi-carrier index keying," *IEEE Commun. Lett.*, vol. 18, no. 10, pp. 1763–1766, Oct. 2014.

[11] T. V. Luong and Y. Ko, "Symbol Error Outage Performance Analysis of MCIK-OFDM over Complex TWDP Fading," in *2017 European Wireless Conf.* VDE, May 2017, pp. 1–5.

[12] ——, "A Tight Bound on BER of MCIK-OFDM With Greedy Detection and Imperfect CSI," *IEEE Commun. Lett.*, vol. 21, no. 12, pp. 2594–2597, Aug. 2017.

[13] ——, "Impact of CSI uncertainty on MCIK-OFDM: Tight closed-form symbol error probability analysis," *IEEE Trans. Veh. Technol.*, vol. 67, no. 2, pp. 1272–1279, Feb. 2018.

[14] E. Başar, "OFDM with index modulation using coordinate interleaving," *IEEE Wireless Commun. Lett.*, vol. 4, no. 4, pp. 381–384, Aug. 2015.

[15] J. Zheng and R. Chen, "Achieving transmit diversity in OFDM-IM by utilizing multiple signal constellations," *IEEE Access*, vol. 5, pp. 8978–8988, Aug. 2017.

[16] J. Choi, "Coded OFDM-IM with transmit diversity," *IEEE Trans. Commun.*, vol. 65, no. 7, pp. 3164–3171, Jul. 2017.

[17] E. Başar, "Multiple-input multiple-output OFDM with index modulation," *IEEE Signal Process. Lett.*, vol. 22, no. 12, pp. 2259–2263, Dec. 2015.

[18] B. Zheng, M. Wen, E. Basar, and F. Chen, "Multiple-input multiple-output OFDM with index modulation: Low-complexity detector design," *IEEE Trans. Signal Process.*, vol. 65, no. 11, pp. 2758–2772, Jun. 2017.

[19] J. Crawford, E. Chatziantoniou, and Y. Ko, "On the SEP analysis of OFDM index modulation with hybrid low complexity greedy detection and diversity reception," *IEEE Trans. Veh. Technol.*, vol. 66, no. 9, pp. 8103–8118, Apr. 2017.

[20] T. V. Luong and Y. Ko, "The BER analysis of MRC-aided greedy detection for OFDM-IM in presence of uncertain CSI," *IEEE Wireless Commun. Lett.*, vol. 7, no. 4, pp. 566–569, Aug. 2018.

[21] T. V. Luong, Y. Ko, and J. Choi, "Repeated MCIK-OFDM With Enhanced Transmit Diversity Under CSI Uncertainty," *IEEE Trans. Wireless Commun.*, vol. 17, no. 6, pp. 4079–4088, Jun. 2018.

[22] I. Al-Nahhal, O. A. Dobre, and S. S. Ikki, "Quadrature spatial modulation decoding complexity: Study and reduction," *IEEE Wireless Communications Letters*, vol. 6, no. 3, pp. 378–381, Jun. 2017.

[23] I. Al-Nahhal, O. A. Dobre, and S. Ikki, "Low Complexity Decoders for Spatial and Quadrature Spatial Modulations-Invited Paper," in *2018 IEEE 87th Vehicular Technology Conference (VTC Spring)*. IEEE, Jun. 2018, pp. 1–5.

[24] I. Al-Nahhal, E. Basar, O. A. Dobre, and S. Ikki, "Optimum low-complexity decoder for spatial modulation," *IEEE Journal on Selected Areas in Communications*, vol. 37, no. 9, pp. 2001–2013, Sept. 2019.

[25] T. V. Luong, Y. Ko, N. A. Vien, D. H. Nguyen, and M. Matthaiou, "Deep Learning-Based Detector for OFDM-IM," *IEEE Wireless Commun. Lett.*, to be published, 2019.

[26] H. L. T. Thanh, V.-D. Ngo, M.-T. Le, and X. N. Tran, "Repeated index modulation with coordinate interleaved ofdm," in *2018 5th NAFOSTED Conf. Infor. and Comput. Science (NICS)*. IEEE, Nov. 2018, pp. 114–118.

[27] H. L. T. Thanh and X. N. Tran, " Performance Analysis of Repeated Index Modulation with Coordinate Interleaving over Nakagami-m Fading Channel," *J. Inf. Commun. Technol., Research and Devel. on ICT*, to be published, 2019.

[28] M. Chiani, D. Dardari, and M. K. Simon, "New exponential bounds and approximations for the computation of error probability in fading channels," *IEEE Trans. Wireless Commun.*, vol. 2, no. 4, pp. 840–845, Jul. 2003.

[29] M. K. Simon and M.-S. Alouini, Digital communication over fading channels. John Wiley & Sons, 2005, vol. 95.

Thi Thanh Huyen Le was born in Hanoi, Vietnam in 1986. She received her B.Eng. and M.Sc. degrees both in Electronic Engineering from Le Quy Don Technical University, Vietnam in 2010 and 2014, respectively. From 2010 to 2016 she was as a lecturer at Le Quy Don Technical University. She recently completed his PhD study and received the PhD degree from Le Quy Don Technical University in 2020. Her research interests consist of MIMO, cooperative communications and index modulation.

Xuan Nam Tran (M'03) is currently a full professor and head of the strong research group on advanced wireless communications, Le Quy Don Technical University. He received his Master of Engineering (ME) in Telecommunications Engineering from University of Technology Sydney, Australia in 1998, and Doctor of Engineering in Electronic Engineering from The University of Electro-Communications, Japan in 2003. From November 2003 to March 2006 he was a research associate at the Information and Communication Systems Group, Department of Information and Communication Engineering, The University of Electro-Communications, Tokyo, Japan. Since 2006 he has been with Le Quy Don Technical University, Vietnam. Prof. Tran's research interests are in the areas of space-time signal processing for communications such as adaptive antennas, space-time coding, MIMO, spatial modulation and cooperative communications. Prof. Tran was a recipient of the 2003 IEEE AP-S Japan Chapter Young Engineer Award, and a co-recipient of two best papers from The 2012 International Conference on Advanced Technologies for Communications and The 2014 National Conference on Electronics, Communications and Information Technology. Prof. Tran is the founding chair and currently the chapter chair of the Vietnam Chapter of IEEE Communications Society. He is a member of IEEE, IEICE and the Radio-Electronics Association of Vietnam (REV).

Vu-Duc Ngo is currently a lecturer at School of Electronics and Telecommunications, Hanoi University of Science and Technology, and a researcher at MobiFone Research and development Center, MobiFone corporation, Vietnam. He received the Ph.D. degree from Korea Advanced Institute of Science and Technology in 2011. During 2007-2009 he was a Cofounder and CTO of Wichip Technologies Inc, USA. Since 2009, he is also a Co-founder and Director of uVision Jsc, Vietnam. Since November 2012 Dr. Ngo has been serving as a BoM member of the National Program on Research, Training, and Construction of High-Tech Engineering Infrastructure of Vietnam. His research interests are in the fields of SoC, NoC design and verification, and VLSI design for multimedia codecs as well as wireless communications PHY layer. Dr. Ngo is the recipient of IEEE 2006 ICCES and IEEE 2012 ATC best paper awards. Dr. Ngo is a member of IEEE.

Minh-Tuan Le was born in Thanh Hoa, Vietnam, in 1976. He received his B.E. degree in Electronic Engineering from Hanoi University of Science and Technology, Vietnam in 1999, M.S. degree and Ph.D. degree both in electrical engineering from Information and Communication University, which is currently the Department of Electrical and Engineering of Korean Advanced Institute of Science and Technology (KAIST), Daejon, Korea, in 2003 and 2007, respectively. From 1999 to 2001 and from 2007 to 2008, he worked as a lecturer at Posts and Telecommunication Institute of Technology (PTIT), Vietnam. From November 2012 to 2015, he worked at Hanoi Department of Science and Technology, Vietnam. He is currently working at MobiFone Reasearch and Development Center, MobiFone Corporation, Vietnam. His research interests include space-time coding, space-time processing, and MIMO systems. Dr. Le is the recipient of the 2012 ATC Best Paper Award from the Radio Electronics Association of Vietnam (REV) and the IEEE Communications Society. He is a member of IEEE.